

Local structure of $\text{In}_{0.5}\text{Ga}_{0.5}\text{As}$ from joint high-resolution and differential pair distribution function analysis

V. Petkov, I-K. Jeong, F. Mohiuddin-Jacobs, Th. Proffen, S.J.L. Billinge

Department of Physics and Astronomy and Center for Fundamental Materials Research, Michigan State University, East Lansing, MI-48823-1116

W. Dmowski

Laboratory for Research on the Structure of Matter and Department of Materials Science and Engineering, University of Pennsylvania, 9201 Walnut Street, Philadelphia, PA 19104
(17 November 1999)

High resolution total and indium differential atomic pair distribution functions (PDFs) for $\text{In}_{0.5}\text{Ga}_{0.5}\text{As}$ alloys have been obtained by high energy and anomalous x-ray diffraction experiments, respectively. The first peak in the total PDF is resolved as a doublet due to the presence of two distinct bond lengths, In-As and Ga-As. The In differential PDF, which involves only atomic pairs containing In, yields chemical specific information and helps ease the structure data interpretation. Both PDFs have been fit with structure models and the way in that the underlying cubic zinc-blende lattice of $\text{In}_{0.5}\text{Ga}_{0.5}\text{As}$ semiconductor alloy distorts locally to accommodate the distinct In-As and Ga-As bond lengths present has been quantified.

61.66.D, 61.72.D, 61.43.Dq

I. INTRODUCTION

Ternary semiconductor alloys, such as $\text{In}_x\text{Ga}_{1-x}\text{As}$, are technologically important because they allow the semiconductor band-gap to be varied continuously between the band-gap values of the end members, GaAs and InAs, by varying the composition, x [1,2]. This has made the technological characteristics, physical properties and structure of $\text{In}_x\text{Ga}_{1-x}\text{As}$ alloys a subject of numerous experimental and theoretical investigations. It has been found that the lattice parameters of the alloys well interpolate between those of the end members which is consistent with the so-called Vegard's law. According to Vegard's law, the structure of alloys adjusts itself so that the individual bond lengths are taking equal, compositionally averaged, values and the bond angles remain unperturbed from their ideal values for any alloy composition. For this reason, all structure dependent properties of $\text{In}_x\text{Ga}_{1-x}\text{As}$ alloys, including electronic band-structure, are often calculated within the virtual crystal approximation (VCA). In this approximation the alloy is assumed to be a perfect crystal with all atoms sitting on ideal lattice sites and site occupancies given by the *average* alloy composition. Both GaAs and InAs have the zinc-blende structure ($F\bar{4}3m$) where In and Ga atoms occupy two interpenetrating face-centered-cubic (fcc) lattices and are tetrahedrally coordinated to each other [3]. Accordingly, the VCA assumes that $\text{In}_x\text{Ga}_{1-x}\text{As}$ alloys have the same zinc-blende structure and, furthermore, the first neighbor interatomic distances (i.e. In-As and Ga-As bonds lengths), bond ionicity, atomic potential etc. take some *average* values for any composition x . However, both extended x-ray absorption fine structure (XAFS) experiments [4] and theory [5] have shown that Ga-As and In-As bonds do not take some *average* value

but remain close to their *natural* lengths $L^o_{\text{Ga-As}} = 2.437 \text{ \AA}$ and $L^o_{\text{In-As}} = 2.610 \text{ \AA}$ in the alloy. This behavior is close to the so-called Pauling model [6] which assumes that the bond length between a given atomic pair in an alloy is more or less a constant, independent on composition x . This finding shows that the zinc-blende lattice of $\text{In}_x\text{Ga}_{1-x}\text{As}$ is significantly deformed to accommodate the two-distinct Ga-As and In-As bond lengths present. Also, the deformation seems to be confined *locally* since the *average* crystal symmetry and structure is still of the cubic zinc-blende type as manifested by the Bragg diffraction patterns.

It is well recognized that *local* structural distortions and associated fluctuations in atomic potentials significantly affect the properties of materials and, therefore, should be accounted for in more realistic theoretical calculations [7]. Thus it seems there is a clear need for more detailed determination of the local structure of $\text{In}_x\text{Ga}_{1-x}\text{As}$ semiconductor alloys which then may be used as an improved quality structure input to theoretical calculations. A number of authors [4,5,8–10] have already proposed model structures for these alloys but there has been limited experimental evidence to date. This prompted us to undertake an extensive experimental study of the local atomic structure of In-Ga-As semiconductor alloys.

The technique of choice for studying the local structure of semiconductor alloys has been XAFS [4,11–13]. However, XAFS provides information about the immediate atomic ordering (first and sometimes second coordination shells) and all longer-ranged structural features remain hidden. To remedy this shortcoming we have taken the alternative approach of obtaining atomic pair distribution functions from x-ray diffraction data.

The atomic pair distribution function (PDF) is the in-

stantaneous atomic number density-density correlation function which describes the atomic arrangement in materials [14]. It is the sine Fourier transform of the experimentally observable total structure factor obtained from a powder diffraction experiment. Since the total structure factor, as defined in Ref. 14, includes both the Bragg scattered intensities and the diffuse scattering part of the diffraction spectrum its Fourier associate, the PDF, yields both the *local* and *average* atomic structure of materials. By contrast an analysis of the Bragg scattered intensities alone, by a Rietveld type analysis [16] for instance, yields the *average* crystal structure only. Determining the PDF has been the approach of choice for characterizing glasses, liquids and amorphous materials for a long time [17]. However, its wide spread application to crystalline materials, where some deviation from the *average* structure is expected to take place, has been relatively recent [18]. The present study is a further step along this line.

Very high real space resolution is required to differentiate the distinct Ga-As and In-As bond lengths present in $\text{In}_x\text{Ga}_{1-x}\text{As}$ alloys. High resolution is attained by obtaining the total structure factor $S(Q)$, where $Q = 4\pi \sin \theta / \lambda$ is the magnitude of the wave vector, to very a high value of Q ($Q > 40 \text{ \AA}^{-1}$). Here, 2θ is the angle between the directions of the incoming and outgoing radiation beams and λ is the wavelength of the radiation used. Recently, we carried out a high energy (60 keV; $\lambda = 0.206 \text{ \AA}$) x-ray diffraction experiment and succeeded in obtaining PDFs for $\text{In}_x\text{Ga}_{1-x}\text{As}$ crystalline materials ($x = 0, 0.13, 0.33, 0.5, 0.83, 1$) of resolution high enough to differentiate Ga-As and In-As first atomic neighbor distances present [19]. An analysis of the experimental data (see Fig. 4 in Ref. [19]) showed that the local disorder in $\text{In}_x\text{Ga}_{1-x}\text{As}$ materials peaks at a composition $x = 0.5$. This observation suggested $\text{In}_{0.5}\text{Ga}_{0.5}$ as the most appropriate candidate for studying the effect of bond-length mismatch on the local structure of In-Ga-As family of semiconductor alloys. An important detail of the high energy experiments carried out is that low temperature (10 K) was used to minimize the thermal vibration in the samples, and hence increase the sensitivity to intrinsic atomic displacements. This left open the question about the impact of temperature on the local structure of $\text{In}_x\text{Ga}_{1-x}\text{As}$ alloys and necessitated the carrying out of an complimentary experiment at temperatures considerably higher than 10 K. To partially compensate for the inevitable loss of resolution from the thermal broadening of atomic pair we carried out an anomalous scattering experiment and determined the In differential PDF at room temperature.

In the present paper we report the high energy low temperature and anomalous scattering (In edge) room temperature experiments on the $\text{In}_{0.5}\text{Ga}_{0.5}\text{As}$. The experimental total and In differential PDFs have been fit with structure models and the way in which the zinc-blende lattice *locally* distorts to accommodate the two distinct Ga-As and In-As bonds present has been quanti-

tified.

II. EXPERIMENTAL DETAILS

A. Sample preparation

The $\text{In}_{0.5}\text{Ga}_{0.5}\text{As}$ alloy was prepared by mixing reagent grade GaAs and InAs powders in the proper amounts. These were sealed under vacuum in quartz tubes. The powders were heated above the liquidus and held for 3 hours to melt them, followed by quenching into cold water. The resulting inhomogeneous alloys were ground, resealed in quartz tubes under vacuum, and annealed at a temperature just below the solidus of the alloy for 72-96 hours. This procedure was repeated until the samples were homogeneous as determined from an x-ray diffraction measurement. The sample for high-energy x-ray diffraction measurements was a thin layer of the powder held between Kapton foils. The thickness of the layer was optimized to achieve a sample absorption $\mu t \sim 1$ for the 60 KeV x-rays. A standard sample holder with a cavity of rectangular shape (2 cm x 4 cm) and depth of 0.5 mm was used with the anomalous x-ray diffraction experiments. The powder was loaded into the cavity to avoid any texture formation and its extended surface left openly exposed to the x-ray beam.

B. High-energy x-ray diffraction experiments

The high resolution total-PDF measurements and data analysis has been reported elsewhere [19,20]. Here, the experiment procedures and data analyses employed are reported in some more detail. The experiments were carried out at the A2 24 pole wiggler beam line at Cornell High Energy Synchrotron Source (CHESS). All measurements were done in a symmetrical transmission geometry at 10 K. The polychromatic incident beam was dispersed using a double crystal Si(111) monochromator and x-rays of energy 60 keV ($\lambda = 0.206 \text{ \AA}$) were employed. An intrinsic Ge detector coupled to a multi-channel (MCA) analyzer was used to detect the scattered radiation. By setting proper energy windows we were able to extract the coherent component of the scattered x-ray intensities during data collection. The diffraction data were collected in scanning at constant ΔQ steps of 0.02 \AA^{-1} . Several runs were conducted and the resulting spectra averaged to improve the statistical accuracy and reduce any systematic error due to instability in the experimental set-up. The diffraction data were smoothed using the Savitzky, Golay procedure [21]. The procedure was tuned in such a way that each data point gained or lost only one Poisson counting standard deviation in the smoothing process. The data were normalized for flux, and corrected for background scattering and experimental effects such as detector deadtime and absorption. The part of

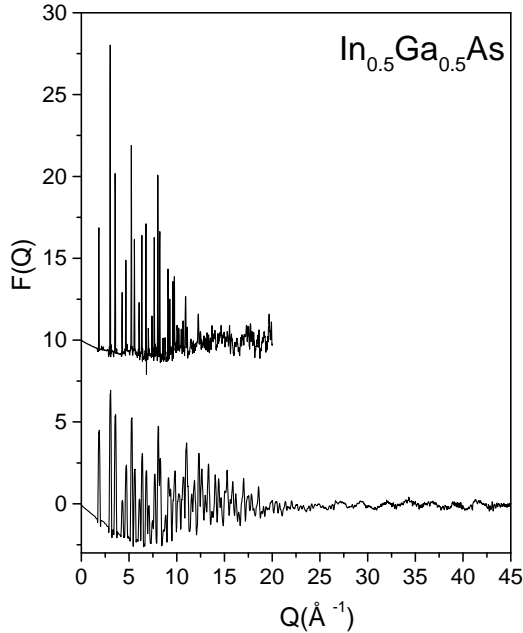


FIG. 1. Total (lower part) and In differential (upper part, offset for clarity) reduced structure factors for $\text{In}_{0.5}\text{Ga}_{0.5}\text{As}$.

Compton scattering at low values of Q not eliminated by the preset energy window was removed analytically applying a procedure suggested by Ruland [22]. The resultant intensities were divided by the square of the average atomic form factor for the sample to obtain the total structure factor $S(Q)$,

$$S(Q) = 1 + \frac{[I^{coh}(Q) - \sum c_i f_i^2(Q)]}{[\sum c_i f_i(Q)]^2} \quad (1)$$

where I^{coh} is the coherent part of the total diffraction spectrum; c_i and $f_i(Q)$ are the atomic concentration and scattering factor of the atomic species of type i ($i = \text{In}, \text{Ga}, \text{As}$), respectively [15,17]. All data processing procedures were done with the help of the program RAD [23]. The reduced structure factor $F(Q) = Q[S(Q) - 1]$ is shown in Fig. 1. As can be seen in the figure the $F(Q)$ data are terminated at $Q_{max} = 45 \text{ \AA}^{-1}$ beyond which, despite the high intensity synchrotron source employed and extra experimental data averaging applied, the signal to noise ratio became unfavorable. It should be noted, however, that this is a very high value of the wavevector for an x-ray diffraction measurement; for comparison Q_{max} achieved with a conventional source such a Cu anode tube is less than 8 \AA^{-1} . The corresponding reduced atomic distribution function, $G(r)$, obtained through a Fourier transform

$$G(r) = 4\pi r[\rho(r) - \rho_o]$$

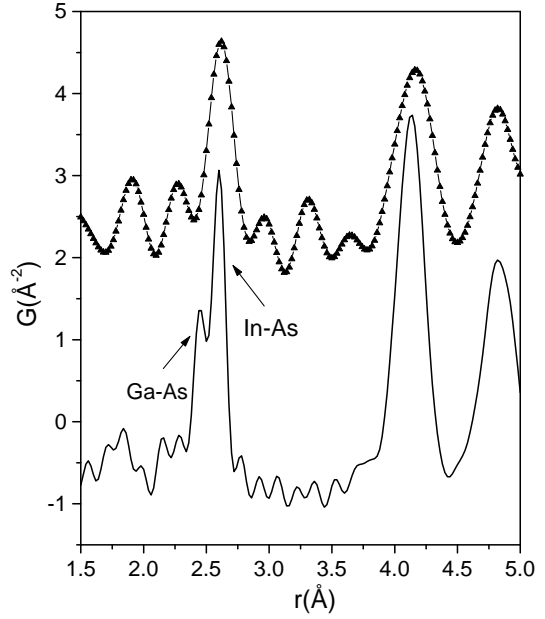


FIG. 2. The reduced total (full line) and In differential (symbols) atomic pair distribution functions for $\text{In}_{0.5}\text{Ga}_{0.5}\text{As}$. The In-differential PDF is significantly broader than the total-PDF because Q_{max} (as shown in Fig. 1), and therefore the real-space resolution of the measured PDF, is much lower.

$$= (2/\pi) \int_{Q=0}^{Q_{max}} Q[S(Q) - 1] \sin Qr \, dQ, \quad (2)$$

is shown in Fig. 2. Here $\rho(r)$ and ρ_o are the *local* and *average* atomic number densities, respectively, and r the radial distance. It should be noted that no modification function, i.e. additional damping of the $S(Q)$ data at high values of Q , was carried out prior to Fourier transformation. This ensures that the data have the highest resolution possible but it results in some spurious ringing in $G(r)$. If Q_{max} is high enough the ringing is small (on the level of the random noise), and in any case it is properly modeled by convoluting $G(r)$ with a Sinc function [33] which we do in all our modeling.

C. Anomalous x-ray diffraction experiments at the In Edge

It is well known that a single diffraction experiment on an n -component system yields a total structure factor which is a weighted average of $n(n+1)/2$ distinct partial structure factors, i.e.

$$S(Q) = \sum_{i,j}^n w_{ij}(Q) S_{ij}(Q), \quad (3)$$

where $w_{ij}(Q)$ is a weighting factor and $S_{ij}(Q)$ the partial structure factor for the atomic pair (i, j) , respectively [15]. The corresponding total PDF, too, is a weighted average of $n(n+1)/2$ partial pair correlation functions. For a multi component system like $\text{In}_{0.5}\text{Ga}_{0.5}\text{As}$ it is therefore difficult to extract information about a particular atomic pair from a single experiment. The combination of a few conventional experiments (let say a combination of neutron, x-ray and electron diffraction experiments) or the application of anomalous x-ray scattering allows the determination of chemical-specific atomic pair distributions.

We briefly describe the use of anomalous scattering to obtain chemical specific PDFs [24]. If the incident x-ray photon energy is close to the energy of an absorption edge of a specific atom in the material, the atomic scattering factor should be considered a complex quantity dependent on both wavevector Q and energy E

$$f(Q, E) = f_o(Q) + f'(E) + i f''(E), \quad (4)$$

where $f_o(Q)$ is the usual atomic scattering factor and f' and f'' are the anomalous scattering terms depending on the x-ray photon energy E . The imaginary term, f'' , is directly related to the photoelectric absorption coefficient and it is small and slowly varying for E below the edge, rises sharply at the edge, and then gradually falls off. f' has a sharp negative peak at the edge with a width which is typically 40-80 eV at half maximum and is small elsewhere [25]. This behavior can be clearly seen in Fig. 3. The anomalous scattering technique takes advantage of the fact that f' and f'' for a particular atomic species change rapidly only within ~ 100 eV of the respective absorption edge and that the characteristic absorption edges for different atomic species are separated by several hundreds of eV. Then a difference of two sets of diffraction data taken at two slightly different energies below an absorption edge of a particular element will contain only a contribution of atomic pairs involving that element. Accordingly, one can define a differential structure factor, DSF, as follows:

$$\text{DSF} = \frac{I(E_1) - I(E_2) - [\Sigma c_i f^2(E_1) - \Sigma c_i f^2(E_2)]}{[\Sigma c_i f(E_1)]^2 - [\Sigma c_i f(E_2)]^2}, \quad (5)$$

where E_1 and E_2 are the two photon energies used [26]. The differential PDF, which gives information about the atomic distribution around the anomalous scattering atoms, is calculated analogous to Eq. (3) with $S(Q)$ replaced by the DSF. Several experiments have already demonstrated the usefulness of anomalous scattering techniques in studying the local atomic ordering in both disordered and crystalline materials [27-29]. A precise knowledge of the anomalous scattering terms is, however, a prerequisite for the interpretation of anomalous scattering experiments. Unfortunately, theoretical models are not capable of providing precise enough values for f' and f'' in the vicinity of absorption edges. That is

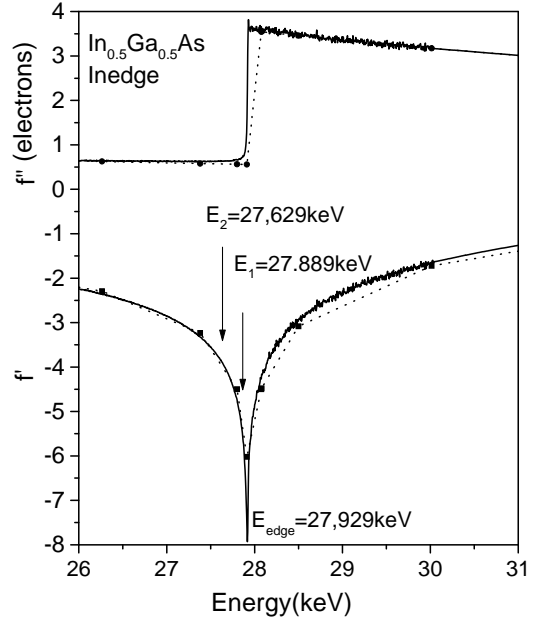


FIG. 3. Energy dependence of the real, f' , and imaginary, f'' , anomalous scattering terms of atomic x-ray scattering factor of In. (Theoretical data - symbols. The dotted line through the symbols is a guide to the eye. Experimental data - full line). The two energies below the In edge used in the present anomalous scattering experiment are marked by arrows.

why anomalous scattering experiments usually involve a complimentary determination of f' and f'' . It is most frequently done by measuring the energy dependence of f'' in the vicinity of the absorption edge and a subsequent determination of f' through the so-called dispersion relation [30]:

$$f'(E_o) = (2/\pi) \int \frac{f''(E)}{[E_o^2 - E^2]} dE \quad (6)$$

The same strategy was adopted in the present anomalous diffraction experiments. These were carried out at the In edge which is the highest energy (~ 27.929 KeV) edge accessible in In-Ga-As system. The experiments were carried out at X7A beam line at the National Synchrotron Light Source at Brookhaven National Laboratory. Two energies, one just below (27.889 KeV), and the other few hundred eV (27.629 KeV) below the In edge were used. The raw data are shown in Fig. 4. A Si channel-cut monochromator was used to disperse the white beam. The monochromator was calibrated by measuring the absorption edge of indium of high purity. The scattered x-rays were detected by a Ge solid state detector coupled to a multi-channel analyzer. Few energy windows, covering several neighboring channels, were set up to obtain counts integrated over specific energy ranges during

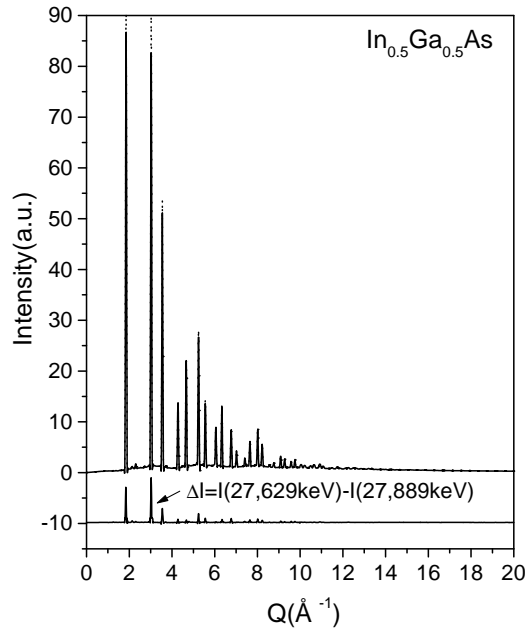


FIG. 4. Coherently scattered intensities of an $\text{In}_{0.5}\text{Ga}_{0.5}\text{As}$ sample measured at two different energies just below the In edge (dots and solid line, respectively). The difference, ΔI , (offset for clarity) between the two data sets is given in the lower part.

the data-collection. These energy windows covered the coherent intensity; coherent, incoherent and In $K\beta$ fluorescence intensities all together; In $K\alpha$ fluorescence; As $K\alpha$ fluorescence, and a window covering the entire energy range which integrates the total scattered intensity in the detector. Integrated counts of these ranges were collected several times and then averaged to improve the statistical accuracy. The data were corrected for detector dead time, Compton and background scattering, attenuation in the sample and residual In $K\beta$ fluorescence which is not possible to be well separated from the coherent component of scattered intensities. In $K\beta$ was determined by monitoring the In $K\alpha$ signal and multiplying it by the ratio of In $K\beta$ to In $K\alpha$ output, which was experimentally determined by a complimentary experiment carried out well above the In edge (~ 29 keV).

By taking the difference between the two data sets, as shown in Fig. 4, all terms that do not involve In were eliminated, because only In scattering factor changed appreciably in the energy region explored while the scattering factors of Ga and As remained virtually the same, and the In DSF was obtained.

The unknown anomalous scattering terms of In, involved in Eq. 5, were determined in the following way: In fluorescence yield was detected by scanning over a wide range across the In edge. The curve was matched to the

theoretical estimates of Chantler [25] for f'' and so the fluorescent yield converted to f'' data. f' was calculated from these f'' data via the dispersion relation as given in Eq. 6. The anomalous scattering terms of In, resulted from the present experiments, are given in Fig. 3. As one can see in the figure, in the vicinity of In edge f' and f'' change sharper than theory predicts. We determined the following values for f' and f'' for the two energies employed: $f' = -3.89$ and $f'' = 0.637$ at $E = 27.629$ keV; $f' = -6.148$ and $f'' = 0.826$ at $E = 27.889$ keV. The use of the experimentally determined but not the theoretically predicted values of f' and f'' turned out to be rather important in obtaining differential structure data of good quality. The In-DSF and differential PDF for $\text{In}_{0.5}\text{Ga}_{0.5}\text{As}$ alloy are shown in Figs. 1 and 2, respectively. The In-DSF appears broader primarily because Q_{max} , and therefore the resolution of the measurement, is much lower than is the case for the total-PDF measurement (as is obvious in Fig. 1). There is an additional broadening of this peak because the In-DSP data were collected at room temperature instead of 10K, but this is expected to be small.

III. RESULTS

As can be seen in Fig. 1 significant Bragg scattering (well defined peaks) is present up to approximately 15 \AA^{-1} in the In difference and total structure factors of $\text{In}_{0.5}\text{Ga}_{0.5}\text{As}$ alloy. At higher wavevectors only an oscillating diffuse scattering is evident. This implies that although the sample still has a periodic structure it contains considerable local displacive disorder. The disorder is due to the mismatch of Ga-As and In-As bond lengths clearly seen as a split first peak in the total PDF of Fig. 2 [19]. Also shown in Fig. 2 is the In difference PDF which has a single first peak well lining up with the higher-r component of the first peak in the total PDF. Since the In differential PDF contains only atomic pairs involving In its first peak can be unambiguously attributed to In-As atomic pairs. This allows us to identify the two components of the first peak in the total PDF as being due to Ga-As and In-As atomic pairs, respectively. According to the present high resolution x-ray diffraction experiments Ga-As and In-As bond lengths in the $\text{In}_{0.5}\text{Ga}_{0.5}\text{As}$ alloy are $2.455(5) \text{ \AA}$ and $2.595(5) \text{ \AA}$ at 10 K, respectively. In the present anomalous diffraction experiments In-As bond length is $2.615(5) \text{ \AA}$ at room temperature. The observed elongation of the In-As bond with temperature is due to the usual thermal expansion observed in materials. We note that the present PDF-based results are in rather good agreement with the XAFS results of Mikkelson and Boyce [4] for Ga-As and In-As bond lengths in $\text{In}_{0.5}\text{Ga}_{0.5}\text{As}$.

An inspection of the experimental PDFs in Fig. 2 (see also Figs. 5 and 6) shows that the nearest atomic neighbor peak is the only one which is relatively sharp. Start-

ing from the second-neighbor peak onwards all atomic-pair distributions (PDF peaks) show significant broadening. The observation shows that the bond-length mismatch gives rise to a considerable deformation of the underlying zinc-blende lattice of $\text{In}_{0.5}\text{Ga}_{0.5}\text{As}$ alloy. To quantify this deformation we explored a few structure models as follows:

A. Supercell model based on the Kirkwood potential

It was previously shown that a 512 atom supercell for the alloy structure, based on the zinc-blende unit cell but with In and Ga randomly arranged on the metal sublattice and atomic positions relaxed using the Kirkwood potential [31], explains well the high-resolution total-PDFs [19]. In addition to this high spatial resolution PDF we now have a PDF which is chemically resolved. We are interested to know whether this supercell model is still sufficient for describing these new data. The model has been described in detail elsewhere [32].

In the present modeling we used the same force constants α_{ij} and β_{ij} that were selected to fit the end members GaAs and InAs [19,32]. Using the relaxed atomic configuration a dynamical matrix has been constructed and the eigenvalues and eigenvectors found numerically. From this the Debye-Waller factors for all the individual atoms in the supercell have been determined. The PDF of the model was then calculated using a Gaussian broadening of the atomic-pair correlations to account for the purely thermal and zero-point motion. The width of the Gaussians was determined from the theoretical Debye-Waller factors [32]. In addition, the calculated PDF was convoluted with a Sinc function to account for the truncation of the data at Q_{max} . [33]. A comparison between the model and experimental results is shown in Fig. 5. The agreement with both the high spatial resolution data (Fig. 5(a)) and with the differential PDF (Fig. 5(b)) is clearly very good. It has already been demonstrated [19] that the Kirkwood-based model well reproduces the displacements of As and metal atoms in In-Ga-As alloys extracted from a model independent analysis the PDF peak widths. Thus the present and previous results suggest that the Kirkwood-based model is a good starting point for any further calculations requiring good knowledge of the local structure of the $\text{In}_{0.5}\text{Ga}_{0.5}\text{As}$ alloy.

B. Refinement of chemically resolved differential and Spatially resolved Total PDF

In this paper we present, for the first time, both high-resolution total- and chemically resolved In-partial PDFs for $\text{In}_{0.5}\text{Ga}_{0.5}\text{As}$. In the previous Section we showed that the data are consistent with a supercell model based on the Kirkwood potential. However, in addition we would

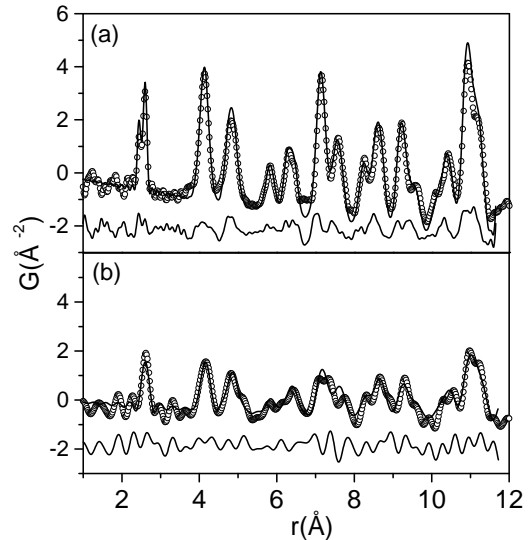


FIG. 5. Experimental (open circles) and model (solid line) PDFs for $\text{In}_{0.5}\text{Ga}_{0.5}\text{As}$ alloy. (a) total PDF; (b) In differential PDF. Model PDFs are based on Kirkwood-type potential minimization. The residual difference between the model and experimental data is given in the lower part.

like to extract structural information from the data without recourse to potential-based models which can be used to compare with other experimental results [4,9,34–38] and theoretical predictions [5,8–10].

To do this we have constructed the simplest possible model that was still consistent with the data, and we have refined it using the PDF profile-fitting program PDF-FIT [42]. We have fit to both the high-spatial resolution total-PDF *and* the chemically resolved differential PDF data at the same time which resulted in equivalent atomic displacement parameters being refined.

The model is based on the 8-atom cubic unit cell of the zinc-blende structure. The split nearest-neighbor peak in the total PDF, and the shifted nearest-neighbor peak in the In-differential PDF, both require that definite static displacements of fixed length be incorporated in the model. In addition, the shifted position of the nearest neighbor peak in the In-differential PDF requires that a model be constructed which has a definite chemical species on specific sites, i.e., goes beyond the virtual crystal approximation. In simple 8-atom cubic unit cell this *de facto* leads to a chemically ordered model that is not observed in the real alloy and which, furthermore, does not sample all of the possible chemical environments for As in the random alloy [9,10,39]. Nonetheless, this is the minimal model which can be successfully refined to

the experimental data to extract information about local atomic displacement amplitudes.

In this model the four metal sites are populated with two In and two Ga ions. Static displacements of As and metal ions were then allowed. The model was constrained so that all four As sites had the same displacement amplitude. The metal sites were likewise constrained to be displaced by the same amount as each other, but the metal site displacement was independent of the As sub-lattice displacement. The directions of the displacements were also constrained to be along $\langle 111 \rangle$ type directions. The choice of which of the 8 possible $\langle 111 \rangle$ directions was determined by the chemical environment. A model with $\langle 100 \rangle$ type displacements was less successful at reconciling the sharp first peak and broad later peaks in the PDF. This is discussed in more detail later. We call these the “discrete” displacements. In addition to the discrete atomic displacements, atomic-displacement-parameters (thermal factors) and lattice parameters were refined. The thermal factors contain both *static* and *dynamic* disorder. These atom displacement distributions we refer to as “continuous” to differentiate from the discrete displacements described above. Finally, the nearest neighbor peak was sharpened with respect to the rest of the PDF using a sharpening factor. This accounts for the highly correlated nature of the displacements of near-neighbor atoms. [40] The resulting fit to the data is shown in Fig. 6.

The values we refine are as follows: the discrete displacements on the As and Metal sublattices are 0.133(5) Å and 0.033(8) Å respectively. These values are independent of temperature. The continuous-displacement amplitudes are $\langle u_{As}^2 \rangle = 0.00814(12)$ Å² and $\langle u_M^2 \rangle = 0.00373$ Å² for the As and metal sublattices at $T = 10$ K and $\langle u_{As}^2 \rangle = 0.0135(15)$ Å² and $\langle u_M^2 \rangle = 0.010(2)$ Å², respectively, at room temperature. These compare with literature values of $\langle u_{As}^2 \rangle = 0.0015(8)$ Å² and $\langle u_M^2 \rangle = 0.0017(9)$ Å² for the end-member compounds at 10 K [19], and $\langle u_{As}^2 \rangle = 0.00716(5)$ Å² and $\langle u_M^2 \rangle = 0.009$ Å² at room temperature [41] for As and the metal site, respectively.

The discrete displacements obtained from the fits are illustrated schematically, by a projection of a fragment of the structure down the [010] direction, in Fig. 7. This shows that both the discrete and continuous displacements (indicated schematically by the size of the circles representing the atoms) are larger on the As than the metal sublattice. The size of the circles representing the continuous-displacements have been exaggerated.

IV. DISCUSSION

Existing experimental results that characterize the structure of semiconductor alloys beyond the average structure include XAFS [4,9,35], ion-channeling [34], x-ray diffuse scattering [36], and Raman scattering [37].

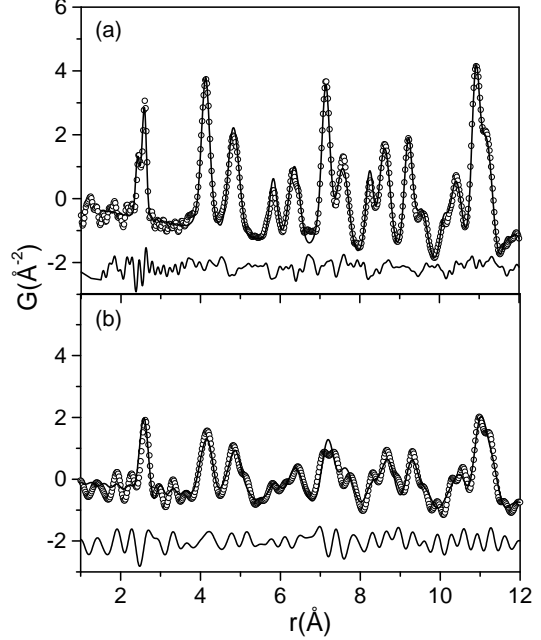


FIG. 6. Experimental (open circles) and model (solid line) PDFs for $\text{In}_{0.5}\text{Ga}_{0.5}\text{As}$ alloy. (a) total PDF; (b) In differential PDF. Model PDFs are based on a distorted zinc-blende-type structure. The residual difference between the model and experimental data is given in the lower part.

The XAFS results clearly show that short and long near-neighbor bonds exist which are from Ga-As and In-As neighbors respectively. The bond-length *distribution* is not recovered with great accuracy and there is limited information available on higher neighbor pairs; however, the indication is that the atom-pair separations return quickly to the virtual crystal values with increasing pair-separation, r . This implies significant distortions to the crystal structure. Indeed, a correct analysis of the phonons in Raman spectra from $\text{Ga}_{1-x}\text{In}_x\text{As}$ required significant structural distortions [37]. Our current and earlier [19] PDF results bear out all these observations.

The discrete displacements refined in our $\langle 111 \rangle$ displaced model are primarily determined by the splitting, and displacement, of the first peak in the total and In-differential PDF’s, respectively: this sharp feature in the PDF is very sensitive to the amplitude of the discrete displacement. The bond-length difference, Δr , between the end-members is 0.173 Å and is ~ 0.14 Å in the alloy [4,19]. If we add the discrete displacements on the arsenic and metal sites we get $\Delta r = 0.16(2)$ Å. The bond-length difference can be obtained directly by fitting Gaussians to the first PDF peak in a model independent way [19]. What this modeling shows is that within the structure, most of the relaxation of local bonds occurs by arsenic moving off its site, but displacements of the

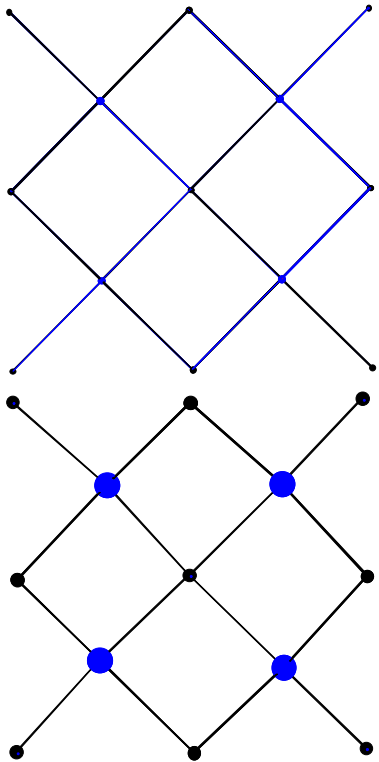


FIG. 7. Schematic representation of the discrete distortions to the zinc-blend structure obtained from the fitting. Fragments from the ideal structure (top panel) can be compared with the distorted (lower panel) structure. The view is a projection along the [010] direction. The large circles are the As sites and the small circles the metal sites. The relative sizes of the circles reflect schematically the relative sizes of the continuous-displacements on each site in the undoped material (top panel) and the alloy (bottom); however, their size has been exaggerated.

metal atoms are also important.

Ion channeling results give a precise determination of the mean-square displacement amplitude, $\langle u^2 \rangle$, (including static and dynamic components) perpendicular to the channeling direction. The results of Haga *et al.* [34] give a $\langle u^2 \rangle$ for $\text{Ga}_{0.47}\text{In}_{0.53}\text{As}$ of 0.017 \AA^2 at room temperature. Based on the theoretical thermal amplitude of the end-member compounds being $\langle u^2 \rangle = 0.0121 \text{ \AA}^2$, (and in good agreement with the value measured using the PDF [20]) they determined that the mean-square static displacements perpendicular to [100] were of magnitude $\langle u^2 \rangle = 0.005 \text{ \AA}^2$. They saw a similar value in directions perpendicular to $\langle 110 \rangle$. This corresponds to a static root-mean-square displacement amplitude of 0.07 \AA . This is much smaller than the discrete displacements of 0.133 \AA that we observe. However, if we find the average displacement by adding the discrete displacements on the As and metal sublattices in quadrature and dividing by 2 we get 0.068 \AA^2 in good agreement with the ion channeling. Their work did not report which sublattice contributed most of the disorder; however, there is a sug-

gestion from electron diffraction [38], in agreement with theory [5,8–10], that the As sublattice is more disordered as we show directly from our measurement.

Finally, we note that the actual displacement pattern on the arsenic site is expected to have $\langle 111 \rangle$ type displacements (as in our model) but also significant $\langle 100 \rangle$ type displacements [9,20,10]. In fact, recent calculations indicate that the $\langle 100 \rangle$ displacements should be significantly more pronounced than $\langle 111 \rangle$ displacements, especially at room temperature [10]. We are undertaking a more sophisticated modeling approach to explore this prediction. We tried a simple $\langle 100 \rangle$ displaced model, analogous to the one described here, but found it to explain the data less successfully than the $\langle 111 \rangle$ model we described. We feel that this is a deficiency of the simple single-displacement-direction modeling rather than signifying that the displacement directions are actually $\langle 111 \rangle$ in the real alloy. The likely reason is that larger displacement amplitudes are required along $\langle 100 \rangle$ directions to satisfy the bond-length difference seen in the first PDF peak (actually $\sqrt{2}$ times larger). With these large discrete displacements it is harder for the model to account for additional disorder in the data using enlarged thermal factors. A better fit in these imperfect models is obtained with smaller discrete displacements coupled with larger continuous-displacements. However, an improved fit should result from a more sophisticated model which includes both $\langle 100 \rangle$ and $\langle 111 \rangle$ type displacements.

V. CONCLUSIONS

From high real space resolution total and In differential PDFs of $\text{In}_{0.5}\text{Ga}_{0.5}\text{As}$ alloy we conclude the following: In good agreement with earlier XAFS results [4] the Ga-As and In-As bonds do not take some compositionally averaged length but remain close to their natural lengths in $\text{In}_{0.5}\text{Ga}_{0.5}\text{As}$ alloy. This bond-length mismatch brings about a considerable local disorder seen as a significant broadening of the next- nearest atomic-pair distributions. The positions and widths of the low and high- r peaks in both the total- and indium differential-PDFs are very well reproduced using a relaxed supercell model based on the Kirkwood potential with parameters taken from fits to the end-members of the alloy series. This suggests that this is a reasonable approach for generating the local structure of these alloys.

A co-refinement of both the high-resolution total PDF and the chemically resolved indium differential PDF using a simplified structural model was carried out. The arsenic sublattice contains most of the disorder in the structure as evidenced from both discrete atomic displacements in the model and enlarged thermal parameters. However, small, but significant, displacements are evident on the metal sites and these have been quantified.

ACKNOWLEDGMENTS

We would like to acknowledge M. F. Thorpe and J. Chung for discussions and for making the results of their supercell calculations available for comparison with the experimental data. We would like to acknowledge S. Kycia and A. Perez for help in collecting the CHESS data. We are very grateful to T. Egami for making x-ray beam-time available to us and to D. E. Cox for help with the NSLS experiments. This work was supported by DOE grant DE FG02 97ER45651. S.J.L.B. also acknowledges support from the Alfred P. Sloan Foundation as a Sloan Fellow. High- energy x-ray diffraction experiments were carried out at Cornell High Energy Synchrotron Source (CHESS). CHESS is operated by NSF through grant DMR97- 13424. Anomalous scattering experiments were carried out at The National Synchrotron Light Source, Brookhaven National Laboratory, which is funded under contract DE-AC02-98CH10886.

[1] J. C. Wooley in *Compound Semiconductors*, eds. R. K. Willardson and H. L. Goering, Reinhold, New York, 1962.

[2] V. Narayananamuri, *Science*, **235**, (1987) 1023.

[3] R.W.G. Wyckoff, *Crystal Structures*, Wiley, New York, 2nd edition, 1967.

[4] J.C. Mikkelsen and J.B. Boyce, *Phys. Rev. Lett.* **49**, (1982) 1412; J.C. Mikkelsen and J.B. Boyce, *Phys. Rev. B* **28** (1983) 7130.

[5] Y. Cai and M.F. Thorpe, *Phys. Rev. B* **46** (1992) 15879.

[6] L. Pauling, *The Nature of the Chemical Bond*, (Cornell University Press, NY, 1967).

[7] A. Zunger et al, *Phys. Rev. Lett.* **65** (1990) 353.

[8] J.L. Martins and A. Zunger, *Phys. Rev. B* **30** (1984) 6217; M.C. Schabel and J. L. Martins *Phys. Rev. B* **43** (1991) 11873.

[9] A. Balzarotti et al. *Phys. Rev. B* **31** (1985) 7526; H. Oyanagi et al. *Solid State Commun.* **67**, (1988) 453.

[10] A. Silverman, A. Zunger, R. Kalish and J. Adler, *Europhys. Lett.* **31**, 373 (1995); A. Silverman, A. Zunger, R. Kalish and J. Adler, *Phys. Rev. B* **51**, 10795 (1995).

[11] J.C. Aubry, T. Tyliszczak, P. Hitchcock, J.-M. Baribeau and T.E. Jackman, *Phys. Rev. B* **59** (1999) 12872.

[12] R. Shioda, K. Ando, T. Hayashi and M. Tanaka, *Phys. Rev B* **58** (1998) 1100.

[13] J.C. Woicik, J.G. Pellegrino, B. Steiner, K.E. Miyano, S.G. Bompard, L.B. Sorensen, T.-L. Lee and S. Khalid, *Phys. Rev. Lett.* **79** (1997) 5026.

[14] B. E. Warren, *X-ray diffraction*, Dover, New York, 1990.

[15] C.N.J. Wagner, *J. Non-Cryst. Solids* **31** (1978).

[16] H. Rietveld, *J. Appl. Crystallogr.* **2** (1969) 65.

[17] Y. Waseda, *The structure of non crystalline materials*, New York: McGraw Hill, 1980.

[18] T. Egami, *Mater. Trans.* **1** (1990) 163; T. Egami in *Local structure from diffraction*, edited by S.J.L. Billinge and M.F. Thorpe p. 1, New York, Plenum. 1998.

[19] V. Petkov, I.-K. Jeong, J. Chung, M.F. Thorpe, S. Kycia and S.J.L. Billinge, *Phys. Rev. Lett.* **83**, 4089 (1999).

[20] I-K. Jeong, V. Petkov, F. Mohiuddin-Jacobs, S. Kycia, S. J. L. Billinge, unpublished.

[21] A. Savitzky and M.J.E. Golay, *Anal. Chem.* **36** (1964) 1627.

[22] W. Ruland, *Br. J. Appl. Phys.* **15** (1964) 1301.

[23] V. Petkov, *J. Appl. Cryst.* **22** (1989) 387.

[24] D. Price and M. L. Saboungi in *Local Structure From Diffraction* edited by S.J.L. Billinge and M.F. Thorpe p. 23, New York, Plenum. 1998.

[25] C. T. Chantler, *J. Phys. Chem. Ref. Data* **24** (1995) 71.

[26] Y. Waseda, in *Novel applications of Anomalous (Resonant) x-ray scattering for structural characterization of disordered materials*, Berlin, Springer-Verlag, 1984.

[27] P. H. Fuoss, P. Eisenberger, W.K. Warburton and A. Bienenstock, *Phys. Rev. Lett.* **46** (1981) 1537.

[28] M. Saito, M. Wakshima, N. sato, T. Fujino, Y. Waseda, E. Matsubara and K. T. Jacob, *Z. Naturforsch.* **49a** (1994) 1031.

[29] X.B. Kan, H. Rennier, J. Quintana, J.L. Peng and J.B. Cohen, *J. Appl. Phys.* **77** (1995) 34.

[30] P. Dreier, P. Rabe, W. Malzfeldt and W. Niemann, *J. Phys. C: Solid State Physics* **17** (1984) 3123.

[31] J.G. Kirkwood, *J. Chem. Phys.* **7** (1939) 506.

[32] Jean S. Chung, M. F. Thorpe, *Phys. Rev. B* **55**, 1545 (1997); *ibid* **59**, 4807 (1999).

[33] S. J. L. Billinge in *Local Structure From Diffraction* edited by S.J.L. Billinge and M.F. Thorpe p. 137, New York, Plenum. 1998.

[34] T. Haga, T. Kimura, Y. Abe, T. Fukui and H. Saito, *Appl. Phys. Lett.* **47**, 1162 (1985).

[35] T. Fukui, *Jpn. J. Appl. Phys.* **23**, L208 (1984).

[36] F. Glas, C. Gors and P. Hénoc, *Philos. Mag. B* **62**, 373 (1990).

[37] G. Landa, *Solid State Commun.* **86**, 351 (1993).

[38] F. Glas and P. Hénoc, *Philos. Mag. A* **56**, 311 (1987).

[39] M. C. Schabel and J. L. Martins, *Phys. Rev. B* **43**, 11873 (1991).

[40] I-K. Jeong, Th. Proffen, F. Mohiuddin-Jacobs and S.J.L. Billinge, *J. Phys. Chem. A*, **103** 921-924, (1999).

[41] J. Stahn, M. Möle and U. Pietsch, *Acta Crystallogr. B* **54**, 231 (1998); U. Pietsch, *Phys. Stat. Sol. B* **107**, 185 (1991).

[42] Th. Proffen and S.J.L. Billinge, *J. Appl. Crystallogr.* **32**, 572 (1999).

